nature genetics

Molecular characterization of clonal interference during adaptive evolution in asexual populations of *Saccharomyces cerevisiae*

Katy C Kao[1] & Gavin Sherlock[2]

The classical model of adaptive evolution in an asexual population postulates that each adaptive clone is derived from the one preceding it[1]. However, experimental evidence has suggested more complex dynamics[2–5], with theory predicting the fixation probability of a beneficial mutation as dependent on the mutation rate, population size and the mutation's selection coefficient[6]. Clonal interference has been demonstrated in viruses[7] and bacteria[8] but not in a eukaryote, and a detailed molecular characterization is lacking. Here we use three different fluorescent markers to visualize the dynamics of asexually evolving yeast populations. For each adaptive clone within one of our evolving populations, we identified the underlying mutations, monitored their population frequencies and used microarrays to characterize changes in the transcriptome. These results represent the most detailed molecular characterization of experimental evolution to date and provide direct experimental evidence supporting both the clonal interference and the multiple mutation models.

In his seminal paper in 1932, Muller proposed that in asexual populations, adaptive events occur in succession[1]. This now classical model of evolution by clonal replacement has been the basis for experimental and theoretical work in microbial population genetics for three quarters of a century[9,10]. Support for this theory has come from studies of *Escherichia coli* populations in which the data are consistent with the complete replacement of the population with an adaptive clone before the appearance of subsequent ones[11]. Further, neutral marker frequency in evolving populations has been used to infer the occurrence and fixation of adaptive events, known as adaptive sweeps[12,13]. However, theory suggests that the chance of fixation of an adaptive mutation is dependent on multiple factors[6,14], and mounting experimental evidence suggests that the classical model of clonal replacement may require substantial modification[2,3,5,8,15]. However, owing to the difficulty of establishing the exact provenance of newly arising adaptive clones, prior studies have focused on the end clones from experimental evolutions[3,16], and no empirical study has clearly characterized and demonstrated the dynamics of the molecular changes underlying adaptive events during evolution. Here, we report the use of different fluorescent markers to visualize the occurrence of specific adaptive events in evolving populations of *Saccharomyces cerevisiae*, which we use to facilitate the detailed molecular characterization of each.

To determine the population structure during adaptive evolution in asexual populations growing in continuous culture, we seeded glucose-limited chemostat cultures with equal numbers of three fluorescently marked otherwise isogenic haploid yeast strains and monitored their relative population sizes by FACS. The data (**Fig. 1a**) show that subpopulations expand at various times during the *in vitro* evolution, suggesting the presence of an adaptive clone within a particular expanding subpopulation. However, these expansion events did not lead to clonal replacement; instead, we observed that a differently colored subpopulation would subsequently expand, and the previously expanding population would contract. In additional experiments (**Fig. 1b**) we observed the same phenomenon, whereby the expansion of subpopulations rarely resulted in clonal replacement and adaptive events typically did not fix in the population.

To further establish the existence of adaptive mutations in the expanding subpopulations, we sorted samples from the population depicted in **Figure 1a** by FACS from generations where an expanding subpopulation reached its maximum proportion. Using pairwise fitness assays, we identified the most-fit adaptive clones from the expanding red, green or yellow subpopulations from generations 56, 91, 196, 266 and 385 (**Fig. 1a** and Methods). These we refer to as M1 through M5 (**Supplementary Table 1** online). Fitness coefficients were used to estimate whether each adaptive subpopulation was comprised solely of its respective adaptive clones (**Fig. 2**). The fitness coefficients showed each adaptive subpopulation, other than that containing M2, isolated at generation 91, to be an impure mixture of adaptive clones and wild-type or less-fit clones, because there were significant differences between the fitness of the adaptive clone and that of the adaptive subpopulation in one or both of the competition experiments shown in **Figure 2**. Although M2 was not more fit than the previous adaptive clone, M1, it was fitter than the original parents. Thus, although M2 was able to outcompete the residual parental population, it was not

[1]Department of Chemical Engineering, Texas A&M University, College Station, Texas 77843, USA. [2]Department of Genetics, Stanford University, Stanford, California 94305, USA. Correspondence should be addressed to G.S. (sherlock@genome.stanford.edu).

Received 15 July; accepted 23 September; published online 23 November 2008; doi:10.1038/ng.280

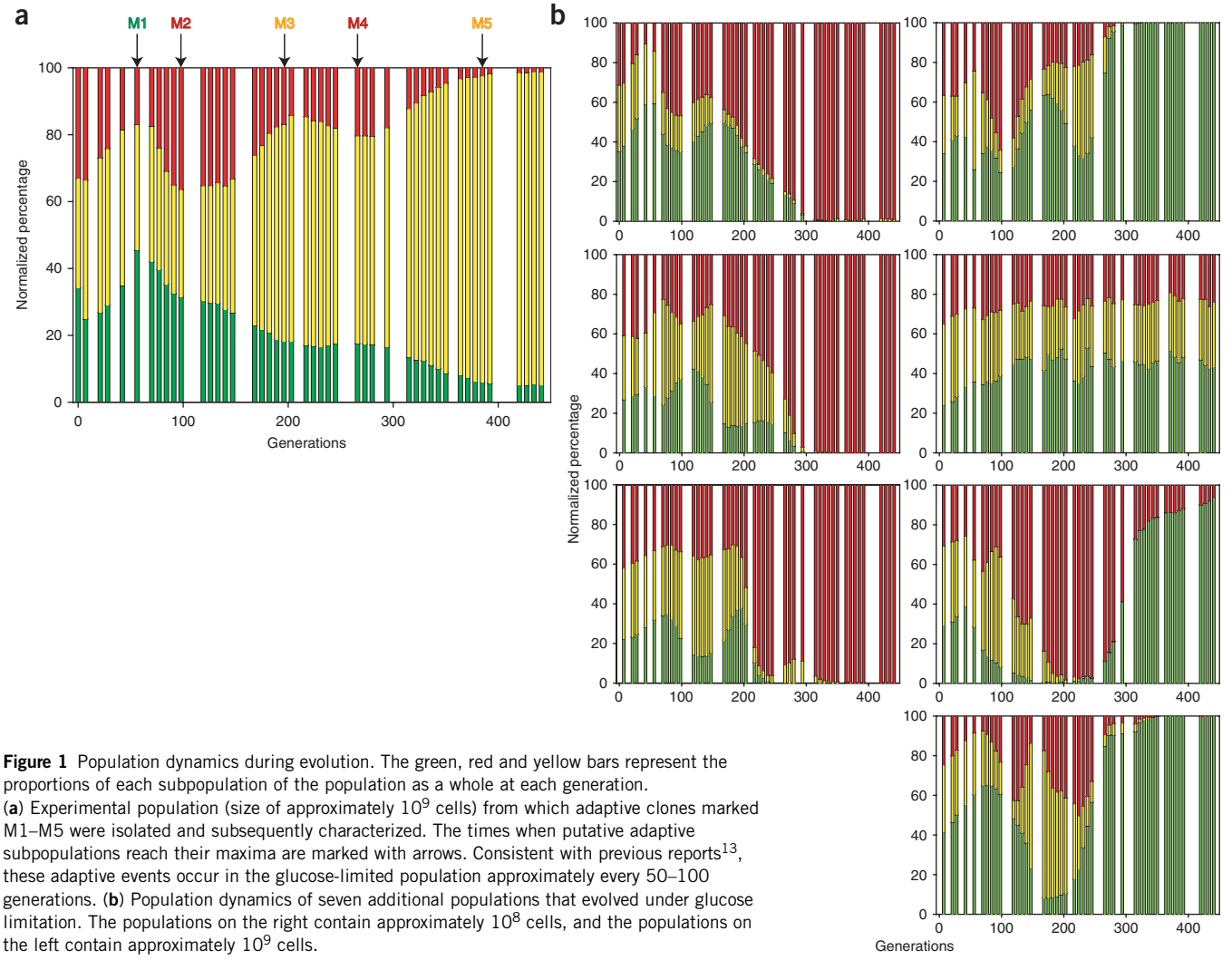

Figure 1 Population dynamics during evolution. The green, red and yellow bars represent the proportions of each subpopulation of the population as a whole at each generation. (**a**) Experimental population (size of approximately 10^9 cells) from which adaptive clones marked M1–M5 were isolated and subsequently characterized. The times when putative adaptive subpopulations reach their maxima are marked with arrows. Consistent with previous reports[13], these adaptive events occur in the glucose-limited population approximately every 50–100 generations. (**b**) Population dynamics of seven additional populations that evolved under glucose limitation. The populations on the right contain approximately 10^8 cells, and the populations on the left contain approximately 10^9 cells.

able to outcompete M1 itself in a direct competition, which is consistent with the data shown in **Figure 1a**.

Single-nucleotide mutations, chromosomal rearrangements, gene duplications and transposon insertions are important evolutionary mechanisms by which adaptation occurs, and examples of all of these have been found in experimental evolution[3,15,17–20]. To investigate the underlying genome changes in our adaptive clones, we used Affymetrix yeast tiling arrays, as described by Gresham *et al.*[21], with modifications (see Methods). A total of nine point mutations, one frameshift mutation, two amplifications and one insertion was observed in clones M1 through M5 (**Table 1**). Clones M2 and M4 share an identical nucleotide change on chromosome 7, strongly suggesting that a succession of adaptive events occurred within the red subpopulation. In the yellow subpopulation, however, the later adaptive clone did not arise from the earlier one, as the mutation observed in M3 was not shared by M5. Thus, just as adaptive events do not always sweep the entire population (**Fig. 1**), the same is true within a subpopulation. Amplifications of the *HXT6/7* locus were observed in the independent lineages M4 and M5. Amplification of this locus has been observed previously[17,18], suggesting that this mutation is adaptive and relatively frequent.

Several mutations observed in the adaptive clones were in genes involved in glucose signaling, either via glucose transport or the protein kinase A (PKA) signaling pathway; this is not surprising, considering that these cultures were grown under glucose-limited conditions. We found two independent mutations involved in the PKA signaling pathway in adaptive clones M3 and M5. The *IRA1* missense mutation found in M3 changes an arginine residue to a lysine; it is unknown how this might affect the activity of the gene product. The *GPB2* mutation in M5 was caused by the insertion of a Ty1 element in the coding region of the gene, likely inactivating its gene product. In addition, a frameshift mutation was observed in *RIm15* in M4, also likely rendering its gene product nonfunctional; RIm15 is a protein kinase conserved in the *Saccharomyces sensu stricto* that acts downstream of and is inhibited by PKA and is involved in nutrient signaling in yeast. From the population frequency data, it is unclear whether the *RIM15* mutation is adaptive (see below). If the *IRA1* mutation is hypomorphic, then both the *GPB2* and *IRA1* mutations would be expected to result in a phenotype that reproduces some aspects of increased signaling through the PKA pathway. Indeed, transcriptome data suggest an increase in PKA signaling in M5 (see **Supplementary Methods** online). In M1, a nonsense mutation was found in the conserved gene *MTH1*, which is involved in the PKA-independent glucose-signaling pathway and negatively regulates transcription of the hexose transporters. The transcriptional profile of M1 showed an increase in expression of the hexose transporters and also

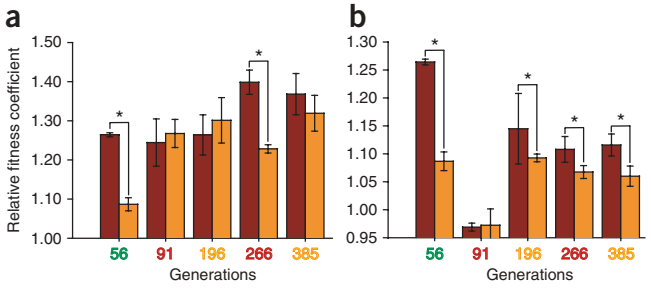

Figure 2 Relative fitness coefficients. (**a**,**b**) Fitness coefficients of adaptive clones (in brown) and adaptive subpopulations (the color of the subpopulation is designated by the color of the generation number under each measurement) from which the adaptive clones were isolated (in orange) versus the original parents (**a**) and the immediately preceding adaptive clone (**b**), measured in triplicate. Error bars, ± 1 s.d. from the mean. Fitness coefficients of adaptive clones that are statistically different from the adaptive subpopulation they were isolated from, as determined using a one-tailed *t*-test with *P* value cutoff of 0.05, are denoted with an asterisk.

suggests an increase in PKA signaling in this clone; a possible cause-and-effect scenario is shown in **Supplementary Figure 1** online.

To determine population frequencies for the mutations, the order of occurrence of the mutations and potentially which mutations are adaptive, we carried out allele-specific RT-PCR[22] on population samples drawn from across the evolutionary time course (**Fig. 3**). These data suggest that in clone M4 the observed mutations in *TAF5*, *RIM15* and the intergenic mutation on chromosome 16 are either not adaptive, or were lost to drift, as their frequencies never reached a detectable threshold. Sequencing of six additional clones at those loci from the generation at which M4 was isolated also showed no evidence of these mutations being present. The population dynamics of the other mutations in M4 suggest that they occurred in the following order: *COX18*, *HXT6/7* amplification and then *MNN4*. In the case of clone M5, it seems that the *HXT6/7* amplification was the first adaptive event, followed by the mutation in *MUK1*, which is currently a gene of unknown function that seems to be strongly adaptive under these conditions. The *GPB2* and *SLY41* mutations started to expand in the population toward the end of the evolution; however, it is currently unclear whether either or both of these mutations are adaptive. Notably, RT-PCR revealed that the *HXT6/7* amplification also arose in the green subpopulation and thus arose independently in all three fluorescently labeled subpopulations. The data strongly suggest that toward the ends of the evolution, the *HXT6/7* amplification had fixed in all three subpopulations, indicating three independent occurrences of this amplification event.

The *MTH1* mutation found in clone M1 was present in the population at low frequency, and, when we sequenced six additional clones from the green population, we did not identify another *MTH1* mutant. This suggests that the observed decline in the green population after generation 56, when the *COX18* mutation was in a higher frequency in the population than the *MTH1* mutation, was most likely due to the loss of residual parental green subpopulation. However, it also suggests that the initial expansion of green was not entirely due to the *MTH1* mutation, as that expansion cannot be solely due to the subpopulation carrying the *MTH1* mutant allele. By the end of the evolution, of the five observed putative adaptive mutations and the additional three independently derived hexose transporter amplifications, only half would likely have survived in the population—those in *MUK1*, *SLY41* and *GPB2*, and the *HXT6/7* amplification in the yellow population (although the adaptive significance of the *SLY41* and *GPB2* mutations is currently unknown), of which only two approach fixation. The other observed adaptive mutations would likely have been lost to clonal interference.

We identified genes whose expression significantly changed (FDR < 1%) between the adaptive clones and the original parents using microarrays (see **Supplementary Methods**). We compared our

Table 1 Genotyping results for adaptive clones analyzed

	Genome modifications					
Clone	Chromosome	Position (bp)	Gene	Mutation	Amino acid residue change	Comment
M1 Green	4	1,014,687	*MTH1*	C to T	Glu338 to stop	Negative regulator of the glucose-sensing signal transduction pathway
M2 Red	7	617,107	*COX18*	T to A	L59H	Mitochondrial inner membrane protein
M3 Yellow	2	521,875	*IRA1*	G to A	R1583K	GTPase-activating protein that negatively regulates Ras
M4 Red	2	616,441	*TAF5*	G to T	G693V	Subunit (90 kDa) of TFIID and SAGA complexes
	4		*HXT6/ HXT7*	Amplification		High-affinity glucose transporter
	6	73,427	*RIM15*	Single-base-pair deletion	Frameshift on codon 333	Glucose-repressible protein kinase
	7	617,107	*COX18*	T to A	L59H	Mitochondrial inner membrane protein
	11	64,698	*MNN4*	A to G	K924E	Putative positive regulator of mannosylphosphate transferase
	16	912,523		T to G		Intergenic
M5 Yellow	1	39,602	*GPB2*	Insertion of ~340 bp from Ty1 LTR		Multistep regulator of cAMP-PKA signaling
	4		*HXT6/ HXT7*	Amplification		High-affinity glucose transporter
	15	893,332	*SLY41*	G to T	W253L	Protein involved in ER-to-Golgi transport
	16	422,266	*MUK1*	C to A	Ser441 to stop	Protein of unknown function; computational analysis of large-scale protein-protein interaction data suggests a possible role in transcriptional regulation

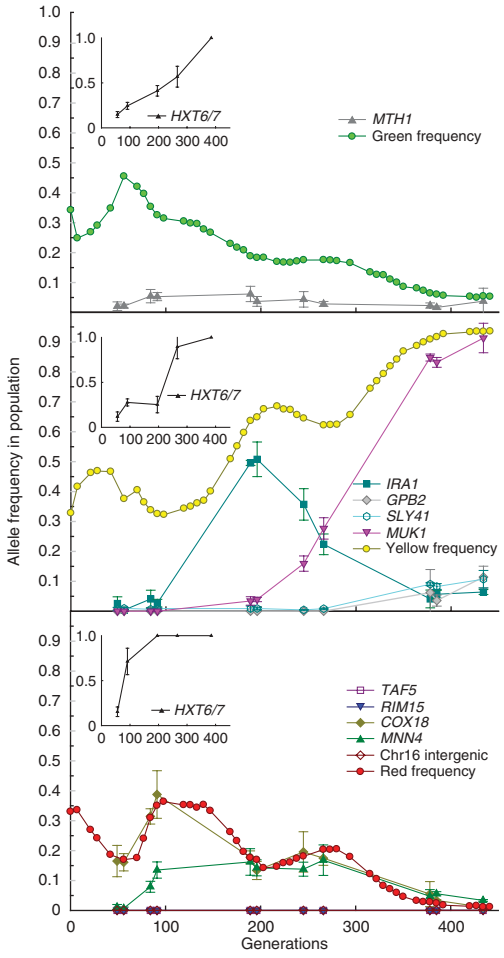

Figure 3 The frequencies of the observed alleles in the entire population and the frequencies of *HXT* amplifications within each of the subpopulations. Green subpopulation, top; yellow subpopulation, middle; red subpopulation, bottom. Because the *HXT6/7* amplification estimation was not as accurate as for the other mutations, and is a measure of the mean copy number within the subpopulation (**Supplementary Methods** and **Supplementary Fig. 4**), it is plotted separately from the other allele frequencies, in the inset boxes. The red, yellow and green circles denote the frequency of those fluorescently labeled subpopulations.

data to those of Wang *et al.*[23], who characterized transcriptional changes in response to increased PKA signaling. In two of our adaptive clones, M1 and M5, the data are consistent with an increase in PKA signaling, as the genes whose expression is either significantly increased or decreased in those clones also show increased or decreased expression, respectively, in their data. An increase in PKA signaling in M5 would be expected, given that Gpb2 is an inhibitor of this pathway, and the M5 mutation in *GPB2* is an insertion that is likely inactivating. However, no mutations were found in the components of the PKA signaling pathway in M1. A possible mechanism may be that the induced hexose transporter gene expression, as a result of the missense mutation in *MTH1*, leads to increased transport of glucose into the cell, which in turn increases the activity of adenylate cyclase, resulting in a more active PKA (**Supplementary Fig. 1**). The occurrence of independent mutations that lead to increased PKA signaling suggests that mutations in this pathway may be readily adaptive under glucose-limited conditions.

In large asexual populations, the occurrence of competing beneficial mutations in the population will interfere with the expansion of an existing adaptive lineage and may result in its elimination. Indeed, this may be the basis for a 'speed limit' that constrains the pace of adaptive evolution in such populations, even when the mutation rate is increased by the presence of so-called 'mutators'[24,25]. All things being equal, clonal interference should increase the complexity of population structure and place limits on the selective advantage of adaptive clones within an evolutionary succession. Clonal interference has been recently incorporated into theoretical models of microbial evolution[6,26,27], and its effects either inferred or observed in experimental studies of *E. coli* and viruses[7,24]. The nonserial occurrences of adaptive events and the incomplete adaptive sweeps observed in our data provide direct support for clonal interference as an important phenomenon in yeast evolving asexually.

A recent multiple-mutation model[28,29] proposed that subsequent adaptive mutations arise within the currently most adaptive clone, even in the presence of clonal interference. Under this multiple-mutations model, we might expect later arising adaptive clones to contain at least one beneficial mutation that occurred on top of a previously observed adaptive clone. Our data indicate that the second observed red adaptive clone, M4, which is the penultimate clone isolated in our experiment, clearly arose from a prior red adaptive clone, M2. However, although the final adaptive clone that we isolated, M5, contains multiple mutations, the only other observable expansion in the yellow subpopulation, M3, is not the founding lineage (**Table 1**). However, the population frequency data clearly establish the presence of multiple adaptive mutations within clone M5, whose expansion was not obvious from the FACS data. The presence of multiple adaptive mutations in clones M4 and M5 supports the theory that multiple mutations are important for adaptive evolution in large populations. Our data provide the most detailed molecular characterization of adaptive evolution in a eukaryote to date and unequivocally demonstrate that in sufficiently large evolving asexual populations of *S. cerevisiae*, the trajectory across the adaptive landscape is determined by clonal interference, rather than clonal replacement.

METHODS

Strains. Yeast strains (**Supplementary Table 2** online) were derived from FY2, a derivative of S288c. We constructed fluorescently tagged strains by integrating plasmids pGS62, pGS63 and pGS64 into FY2 (see **Supplementary Methods**).

Evolution experiments. We inoculated 30 ml chemostat vessels with equal numbers of each fluorescently marked yeast strain in 20 ml. The populations were evolved at steady state under glucose-limited conditions (0.08% glucose in Delft minimal medium) at 30 °C with a dilution rate of 0.2 h^{-1}. The proportion of each fluorescently marked subpopulation was monitored by FACS. We determined that the FACS data were reproducible (**Supplementary Fig. 2** online) and that none of the different colored populations had a significant advantage or disadvantage in either serial batch or short-term continuous cultures (**Supplementary Fig. 3** online).

Identification and isolation of each adaptive mutant. On the basis of the population dynamics (**Fig. 1a**), we determined which of our samples should have a substantial fraction of an adaptive clone in one of the fluorescently marked subpopulations, and we then separated out the sample using FACS. Seven independent colonies were picked from each sorted sample for fitness measurements.

Each clone was competed in continuous culture against the previous adaptive mutant and the clone with highest fitness coefficient was chosen as the adaptive clone. In the case of the red subpopulation from generation 91, none of the clones showed a fitness advantage compared to the preceding green-marked adaptive clone. We compared these red clones against the

original parent and determined that they were all similarly fitter, and picked one arbitrarily as the adaptive clone.

Pairwise competition experiments. Chemostat experiments in 0.08% glucose Delft minimal medium were started with equal numbers of each of the two clones to be competed, which had different fluorescent markers at a dilution rate of 0.2 h^{-1} at 30 °C. In the case of competition involving the adaptive subpopulation, we used a mixture of cells patched on 2% glucose minimum medium plates. Samples were taken every ~8–15 h and the culture compositions were measured by FACS. We plotted the rate of expansion of the fitter strain on a semi-log scale, and calculated the fitness coefficient at the linear range of expansion as

$$s = \frac{\ln\left(\frac{x(t_2)}{y(t_2)}\right) - \ln\left(\frac{x(t_1)}{y(t_1)}\right)}{\Delta t}$$

where x is the normalized proportion of the fitter clone, y is the normalized proportion of the less fit clone, Δt is the difference in generations between t_2 and t_1, and s is the differential growth rate per generation between the two clones. The relative fitness coefficient is $(1 + s)/1$. Experiments were repeated at least three times.

Mutation analysis. We used Affymetrix Yeast tiling v1.0R arrays for finding mutations in the evolved strains by comparing the data for the evolved strains and the parent strains. Only the perfect match (PM) data from the resulting CEL files were used for analysis. Probes that span repeated regions or transposable elements were filtered out. We computed normalization factors for each chromosome by averaging the signals for all the probes (after filtering) in each strain. The difference between the $\log_2$-transformed average signal for each chromosome in the two strains was used as a normalization factor. For each unfiltered probe, the $\log_2$ ratios of the evolved strain over parent strain intensities were calculated, and normalized using the difference calculated above for the appropriate chromosome. For each chromosome, a value, j, for chromosome position i was calculated by averaging the normalized $\log_2$ ratios of probes between positions $i + 6$ to $i + 18$. We identified potential single-base mutations or deletions by looking for at least four consecutive j's whose values were less than the mean minus 3 s.d. (the s.d. was calculated for the whole chromosome). Potential amplifications were identified by a long stretch of consecutive j's, whose values were greater than the mean plus 3 s.d.

Sequencing. Potential mutations were validated by Sanger sequencing using the parental strains as negative controls (primers are listed in **Supplementary Table 3** online).

Population allelic frequency determination. We determined the population frequencies of identified mutations by kinetic PCR[22] using either the iCycler (Bio-Rad Laboratories) or the ABI 7900HT (Applied Biosciences). Each reaction mixture consisted of 20 ng (iCycler) or 10 ng (ABI 7900HT) of total genomic DNA, 0.5 μM primers, and either iQ SYBR Green Supermix (iCycler; Bio-Rad) or iTaq SYBR Green Supermix with ROX (ABI 7900HT; Bio-Rad) in final reaction volume of 20 μl (iCycler) or 10 μl (ABI 7900HT). The reaction conditions were as follows: iCycler (95 °C for 3 min followed by 40 cycles of 95 °C for 20 s, 63 °C for 20 s, 72 °C for 20 s) and ABI 7900HT (95 °C for 3 min followed by 40 cycles of 95 °C for 15 s, 60 °C for 1 min). The approximate frequency of the *HXT6/7* amplification was only determined from the sorted subpopulations. The calculations for the frequencies of the *HXT6/7* amplification in the subpopulations were based on a copy number of 8 for this region. The primers used are listed in **Supplementary Table 3**. Control experiments demonstrating the abilities of the primers to distinguish between the two different alleles are shown in **Supplementary Figure 4** online.

RNA purification and gene expression analysis. Single colonies were used to inoculate overnight cultures in 2% glucose Delft minimal medium grown at 30 °C, which were then used to inoculate glucose-limited chemostat cultures. Cells were harvested approximately 48 h after inoculation, filtered using 0.45 μm analytical test filter funnels (Nalgene), snap-frozen in liquid nitrogen and stored at –80 °C for RNA purification at a later time. Each experiment was repeated three times.

RNA was extracted using a hot acid phenol method and total RNA was eventually resuspended in nuclease-free water. Using the Low RNA Input Linear Amplification Kit, Two-Color (Agilent), we labeled 375 ng of purified total RNA and RNA Spike-In control (Agilent) with either 6 nmol of Cy3-CTP or Cy5-CTP (GE Healthcare) and hybridized them to Agilent 8x15k yeast catalog arrays, which were then washed and scanned. Feature Extraction v 9.1.5 (Agilent) was used to normalize the data using the Spike-In controls.

To identify differentially expressed genes, we analyzed each set of data using the software Significance Analysis of Microarray[30] in a one-class analysis. A delta value was chosen to obtain a set of statistically differentially regulated genes with a false-discovery rate of approximately 1%.

Accession codes. NCBI GEO: microarray expression data are available under accession GSE11071.

Note: Supplementary information is available on the Nature Genetics website.

ACKNOWLEDGMENTS

This work was supported by US National Institutes of Health grants R01 HG003328 (G.S.) and F32 GM079113 (K.C.K.). We thank J. Ying for help with sample handling, E. Tanner for carrying out some of the gene expression microarray experiments, H. Tang for discussions on experimental design, J. Horecka for help with RT-PCR and F.Rosenzweig, B. Dunn and A. Sidow for comments on the manuscript.

AUTHOR CONTRIBUTIONS

K.C.K. and G.S. conceived of and designed this study. K.C.K. performed all experiments and analyses. K.C.K. and G.S. wrote the manuscript.

Published online at http://www.nature.com/naturegenetics/
Reprints and permissions information is available online at http://npg.nature.com/reprintsandpermissions/

1. Muller, H.J. Some genetic aspects of sex. *Am. Nat.* **66**, 118–138 (1932).
2. Helling, R.B., Vargas, C.N. & Adams, J. Evolution of *Escherichia coli* during growth in a constant environment. *Genetics* **116**, 349–358 (1987).
3. Notley-McRobb, L. & Ferenci, T. The generation of multiple co-existing mal-regulatory mutations through polygenic evolution in glucose limited populations of *Escherichia coli*. *Environ. Microbiol.* **1**, 45–52 (1999).
4. Notley-McRobb, L. & Ferenci, T. Experimental analysis of molecular events during mutational periodic selections in bacterial evolution. *Genetics* **156**, 1493–1501 (2000).
5. Rosenzweig, R.F., Sharp, R.R., Treves, D.S. & Adams, J. Microbial evolution in a simple unstructured environment—genetic differentiation in *Escherichia coli*. *Genetics* **137**, 903–917 (1994).
6. Gerrish, P.J. & Lenski, R.E. The fate of competing beneficial mutations in an asexual population. *Genetica* **103**, 127–144 (1998).
7. Miralles, R., Gerrish, P.J., Moya, A. & Elena, S.F. Clonal interference and the evolution of RNA viruses. *Science* **285**, 1745–1747 (1999).
8. Hegreness, M., Shoresh, N., Hartl, D. & Kishony, R. An equivalence principle for the incorporation of favorable mutations in asexual populations. *Science* **311**, 1615–1617 (2006).
9. Crow, J.F. & Kimura, M. Evolution in sexual and asexual populations. *Am. Nat.* **99**, 439–450 (1965).
10. Paquin, C. & Adams, J. Relative fitness can decrease in evolving asexual populations of *S. cerevisiae*. *Nature* **306**, 368–371 (1983).
11. Atwood, K.C., Schneider, L.K. & Ryan, F.J. Periodic selection in *Escherichia coli*. *Genetics* **37**, 146–155 (1951).
12. Novick, A. & Szilard, L. Experiments with the chemostat on spontaneous mutations of bacteria. *Proc. Natl. Acad. Sci. USA* **36**, 708–719 (1950).
13. Paquin, C. & Adams, J. Frequency of fixation of adaptive mutations is higher in evolving diploid than haploid yeast populations. *Nature* **302**, 495–500 (1983).
14. Kim, Y. & Orr, H.A. Adaptation in sexuals vs. asexuals: clonal interference and the Fisher-Muller model. *Genetics* **171**, 1377–1386 (2005).
15. Adams, J. & Oeller, P.W. Structure of evolving populations of *Saccharomyces cerevisiae* adaptive changes are frequently associated with sequence alterations involving mobile elements belonging to the Ty family. *Proc. Natl. Acad. Sci. USA* **83**, 7124–7127 (1986).
16. Herring, C.D. *et al.* Comparative genome sequencing of *Escherichia coli* allows observation of bacterial evolution on a laboratory timescale. *Nat. Genet.* **38**, 1406–1412 (2006).
17. Brown, C.J., Todd, K.M. & Rosenzweig, R.F. Multiple duplications of yeast hexose transport genes in response to selection in a glucose-limited environment. *Mol. Biol. Evol.* **15**, 931–942 (1998).
18. Dunham, M.J. *et al.* Characteristic genome rearrangements in experimental evolution of *Saccharomyces cerevisiae*. *Proc. Natl. Acad. Sci. USA* **99**, 16144–16149 (2002).

19. Segre, A.V., Murray, A.W. & Leu, J.Y. High-resolution mutation mapping reveals parallel experimental evolution in yeast. *PLoS Biol.* **4**, e256 (2006).
20. Blanc, V.M. & Adams, J. Evolution in *Saccharomyces cerevisiae*: identification of mutations increasing fitness in laboratory populations. *Genetics* **165**, 975–983 (2003).
21. Gresham, D. *et al.* Genome-wide detection of polymorphisms at nucleotide resolution with a single DNA microarray. *Science* **311**, 1932–1936 (2006).
22. Germer, S., Holland, M.J. & Higuchi, R. High-throughput SNP allele-frequency determination in pooled DNA samples by kinetic PCR. *Genome Res.* **10**, 258–266 (2000).
23. Wang, Y. *et al.* Ras and Gpa2 mediate one branch of a redundant glucose signaling pathway in yeast. *PLoS Biol.* **2**, e128 (2004).
24. de Visser, J.A.G.M. & Rozen, D.E. Clonal interference and the periodic selection of new beneficial mutations in *Escherichia coli*. *Genetics* **172**, 2093–2100 (2006).
25. de Visser, J.A.G.M., Zeyl, C.W., Gerrish, P.J., Blanchard, J.L. & Lenski, R.E. Diminishing returns from mutation supply rate in asexual populations. *Science* **283**, 404–406 (1999).
26. Gerrish, P. The rhythm of microbial adaptation. *Nature* **413**, 299–302 (2001).
27. Rozen, D.E. & de Visser, J.A.G.M. & Gerrish, P.J. Fitness effects of fixed beneficial mutations in microbial populations. *Curr. Biol.* **12**, 1040–1045 (2002).
28. Desai, M.M. & Fisher, D.S. Beneficial mutation-selection balance and the effect of linkage on positive selection. *Genetics* **176**, 1759–1798 (2007).
29. Desai, M.M., Fisher, D.S. & Murray, A.W. The speed of evolution and maintenance of variation in asexual populations. *Curr. Biol.* **17**, 385–394 (2007).
30. Tusher, V.G., Tibshirani, R. & Chu, G. Significance analysis of microarrays applied to the ionizing radiation response. *Proc. Natl. Acad. Sci. USA* **98**, 5116–5121 (2001).